Materials Research Express

PAPER

Evaluation of the reheating behavior of the cooling slope cast A356 and A380 aluminum alloys

To cite this article: Serhat Acar *et al* 2019 *Mater. Res. Express* **6** 1265c7

View the article online for updates and enhancements.



IOP ebooks™

Bringing you innovative digital publishing with leading voices to create your essential collection of books in STEM research.

Start exploring the collection - download the first chapter of every title for free.

This content was downloaded from IP address 95.183.138.168 on 07/01/2020 at 07:12

Materials Research Express

PAPER

Evaluation of the reheating behavior of the cooling slope cast A356 and A380 aluminum alloys

Serhat Acar, Nazim Acici and Kerem Altug Guler

Yildiz Technical University, Department of Metallurgical and Materials Engineering, Davutpasa Campus, 34210, Esenler, Istanbul, Turkey

E-mail: seacar@yildiz.edu.tr **and** serhatacar63@hotmail.com

Keywords: cooling slope casting, semi-solid reheating, A356 alloy, A380 alloy

RECEIVED
13 September 2019

REVISED
2 November 2019

ACCEPTED FOR PUBLICATION
16 December 2019

PUBLISHED
8 January 2020

Abstract

A356 and A380 alloys are two well-known hypoeutectic Al-Si casting alloys in the non-ferrous casting industry and drew significant attention for semi-solid applications. The cooling slope casting method for producing materials with non-dendritic microstructure is one of the simplest liquid route techniques. In the beginning, microstructural differences of both alloys produced with 30° and 60° tilt angles were examined. It was observed that the angle change has a limited effect on A380 and it is almost non-effective for A356 as-cast structures. The samples were then subjected to the reheating processes for different times and the effects were investigated by measuring the average shape factor and the grain size values. In addition to the natural grain growth, it is understood that the changes in the eutectic are also effective on the properties. The rapid solidification of the melted eutectic by quenching the reheated samples modified the eutectic structure and improved the hardness. On the other hand, grain growth reduces hardness naturally. Additionally, it was observed that the increase in sphericity was supported by the liquid phase formation and it was determined that A356 alloy was more sensitive to reheating and formed larger grains than A380 alloy for the same reheating periods.

1. Introduction

Semi-solid metal processing (SSMP) techniques have attracted a serious amount of attraction since the discovery of thixotropic behaviors of certain metallic alloys in the early 70 s [1, 2]. These techniques base on the basic principles of forming materials between their liquidus and solidus temperatures and consist of two main steps such as the production of appropriate feedstock and final forming into the desired shape at the semi-solid temperature range [3, 4].

Feedstock materials with fine and globular microstructure are essential for further forming processes in the semi-solid state. Thus, the raw material production step is emphasized as the most vital part of the SSMP methods in many pieces of research [5–7]. There are mainly two different routes for obtaining these intermediate materials with desired microstructural properties; liquid state and solid-state routes [8]. In the liquid state routes, non-dendritic feedstock production is provided by either the fragmentation of dendrites due to shear forces or repressing the conditions that necessary for dendritic growth such as constitutive supercooling [9]. On the other hand, the solid-state routes require pre-deformed feedstocks and these kinds of methods are very viable for wrought alloys because feedstocks are usually provided in the deformed state in the first place. During the reheating step in the semi-solid temperature range, deformed grains recrystallize with the spheroidal morphology and the liquid fraction forms at the boundaries of the recrystallized grains in the solid-state routes [10, 11].

Cooling slope (CS) casting has drawn significant attention in recent years as one of the simplest methods among all liquid state routes. In this technique, a low superheated molten alloy is poured over an inclined cooling plate. Fragmentation of the dendritic arms by gravitational forces along the slope, later on, their following detachment and drift into the mold by the motion of liquid metal is the main theory about the formation of equiaxed grains with this method [12–15]. Features like low equipment requirement, simplicity,

© 2020 IOP Publishing Ltd

and cost-effectiveness of this process make it very appealing, however, the microstructure of the final product strictly related to the process parameters such as slope length, slope angle, casting temperature and reheating time prior to forming step [16]. The multiplicity of independent variables renders the control of the process very difficult. Even a slight change in any process parameter may influence the resulting microstructure heavily [17]. Therefore, the optimization of CS casting parameters is essential for producing feedstocks with desired microstructural properties.

Khosravi *et al* [18] investigated the effects of the cooling length, the casting temperature, the tilt angle, and the isothermal holding time on CS cast A356 alloy with an experiment set generated by D-optimal design of the experiment. Three different values were selected for each variable in order to model the effects of the selected variables on the sphericity of obtained microstructures. According to the performed ANOVA test, it has been found casting temperature is the most important factor affecting the globularity of primary Al crystals and the optimum process parameters are found to be the casting temperature of 660 °C, the cooling distance of 360 mm, the tilt angle of 48, and the holding time of 9 min.

Haga *et al* [19] reported that the cooling rate of the ingot in the mold is the most important factor for obtaining a globular microstructure amongst the parameters like casting temperature, cooling length and reheating temperature for Al −6 wt% Si alloy. It was observed that a high cooling rate in the mold-induced spheroidization of primary crystals after remelting step.

On the other hand, according to Legoretta *et al* [20] high thermal conductivity mold gives a fine primary size in the center but also an inhomogeneous microstructure across the ingot of A356 alloy. Researchers also concluded that without the employment of CS, primary crystals tend to be coarser and more dendritic. They also revealed that the tilt angle has only little effect on the final microstructure for low superheats.

Birol [21] examined the microstructural properties of CS cast A357 alloy with the casting temperatures between 620 and 640 °C, cooling lengths between 200 and 400 mm, and reheating times between 5 and 15 min. It was reported that the dendritic primary phase of conventional casting product has successfully transformed into a spheroidal one by the employment CS for every condition that was tested. The effects of the pouring temperature and the cooling length were not evident on the reheated specimens' microstructure. On the other hand, globular grain morphology was attained after only 5 min of reheating, with longer holding times grain coarsening reached high levels.

Das *et al* [22] also conducted a study for modeling the effects of CS casting parameters on the sphericity of A356 alloys microstructure by using Taguchi experiment of design for three levels of the slope angle, the pouring temperature, the wall temperature, and the cooling distance. The optimum processing condition has been determined for 0.83 sphericity index as a slope angle of 60°, pouring temperature of 650 °C, wall temperature of 60 °C and cooling distance of 500 mm.

Samat *et al* investigated the thixoformability of the modified and unmodified A319 alloys. The non-dendritic feedstocks were produced by using a stainless steel CS plate. Both feedstocks were successfully produced within acceptable shape factor and grain size values, i.e. 0.7–0.8 and 50–60 μm. In addition, modified alloy displayed better thixoformability [23].

Kolahdooz *et al* [24] examined the effects of the different CS casting parameters such as the residence time on the slope, solid fraction of the slurry, strain rate and turbulence by using simulations. According to their results, in order to obtain the best microstructural properties, the duration of the slurry on the plate must be enough, and the strain and turbulence must be as high as possible.

In this study, semi-solid slurries of two different aluminum casting alloys which are widely used in the automotive industry, A356 and A380, were produced with CS casting and reheating processes. Castings were operated at 20 °C above of liquidus temperatures of these two alloys with employing a copper slope with a length of 650 mm. Two different levels were examined for the tilt angle i.e., 30° and 60°, and four different reheating times in a wide range of 20 to 80 min were scanned at 20 °C below of the liquidus temperature of both alloys. Microstructures were investigated by means of calculating shape factor and grain size of primary crystals and the findings were reported.

2. Methods

A356 and A380 ingots supplied from a local commercial manufacturer were used in melting processes and the chemical compositions of these alloys are given in table 1. Melting and casting temperatures were determined as 20 °C above the liquidus temperature of both alloys; 635 °C and 615 °C for A356 and A380 alloys, respectively. It was observed that these temperatures contain a minimum amount of superheat for a successful casting process with the available equipment.

In the casting process, a copper tube of 650 mm length and 50 mm diameter was used as a cooling slope and the liquid metal was poured through this tube into a cylindrical steel mold with a diameter of 40 mm. The inner

Table 1. Chemical compositions of A356 and A380 aluminum alloys (mass fraction %).

*	Si	Fe	Cu	Mn	Mg
A356	7.288	0.144	0.011	0.028	0.354
A380	8.220	0.686	3.586	0.189	0.222
*	Zn	Ni	Ti	Pb	Al
A356	0.008	0.0031	0.123	0.0117	Bal.
A380	0.952	0.124	0.037	0.0806	Bal.

surface of the tube was coated with hexagonal boron nitride spray to facilitate metal flow and prevent possible reactions. Tilt angles of castings were preferred as 30° and 60°. The pieces cut from the supplied ingots were melted in clay/graphite crucibles using a resistance type furnace and 1 kg of metal was poured each time for feedstock production. The residual shells remaining in the slope during casting processes were negligible. 40 mm length samples were cut from cast bars for reheating processes. The samples were quenched in the water after the reheating periods of 20, 40, 60 and 80 min in order to freeze the existing microstructure. The reheating temperatures were selected, 20 °C below of the liquidus temperatures of the alloys as 595 °C for the A356 alloy and 575 °C for the A380 alloy. Samples were sectioned for microstructural studies and subjected to the metallographic preparation processes and finally etched with a 0.5% HF solution. Microstructural investigations were performed by Nikon Eclipse MA100 light metal microscope with image analysis support. The obtained microstructures were investigated by calculating the shape factor and grain size values for each specimen. Microstructures of the as-cast specimens were investigated by scanning electron microscope (SEM, Hitachi SU3500 T2) with energy dispersive x-ray spectrometry (EDS, Oxford XACT) for determining the elemental composition of the phases. Formed phases were further evaluated by x-ray diffraction analysis (XRD, Philips PW 3710) using CuKα radiation over 2θ range of 20°–90°. In addition, the hardness of the samples was measured by the universal Brinell hardness tester using 62.5 kg load and 2.5 mm diameter indentation tip.

3. Results and discussion

Microstructures of as-cast bars obtained by CS castings were investigated before reheating. General views of the as-cast microstructures are shown in figures 1 and 2 for both tilt angles. The grain size values, shape factor and additionally measured hardness values are given in table 2. The shape factor and the grain size values were calculated with the formulations given below, where A and P represent grain area and perimeter, respectively.

$$\textbf{\textit{Shape factor}} = 4\pi A/\boldsymbol{P}^2 \quad (1)$$

$$\textbf{\textit{Grain size}} = (4\boldsymbol{A}/\boldsymbol{P})^{1/2} \quad (2)$$

Typical hypoeutectic Al-Si casting alloy structure can be seen in micrographs with light-colored α-Al and dark-colored eutectic zones but with non-dendritic morphology. CS casting successfully suppressed the dendritic solidification of the α-Al phase for both alloys. In as-cast structures, A356 alloy has relatively higher shape factor values, while the A380 alloy has finer grain size. It was also observed that the difference in tilt angle did not cause any significant difference in the grain size of A356 alloy, whereas 60° of tilt angle caused a texture with finer grain structure for A380 alloy.

In both alloys, the main eutectic reaction occurs at 567 °C–568 °C range. Primary aluminum (α-Al) formation begins at 610 °C for A356 alloy and at 594 °C for A380 alloy [25]. Having a wider difference between the main eutectic reaction and the α-Al formation in the A356 alloy allows a further increase in the size of α-Al grains. Therefore, in the casting structures, the grain size of the A356 alloy is slightly higher. Furthermore, this growth time difference before eutectic solidification increases the shape factor of A356 alloy.

There are two different effective mechanisms for the nucleation of initial crystals by CS casting. The first one is the high cooling rate of liquid and the second one is the shear forces caused by the slope to break the growing dendrites. In high tilt angle castings, it is normal to expect the longer contact duration to cooler to decrease when the shear force increases, and vice versa. According to the results inferred from figure 1, none of these mechanisms dominated the other one for A356 alloy and consequently, the grain size was not affected by the difference in the casting angle. On the other hand, this situation was not observed in A380 alloy, and castings with 60° of the tilt angle resulted in slightly finer grain morphology. It can be said that the shear force mechanism to be more effective for this alloy. The underlying reason for this situation is the fluidity of the A380 alloy. The fluidity of A380 alloy is higher due to its greater Si content, and this relative higher fluidity increases the effective shear force during CS casting through the slope and final particle size ends up finer.

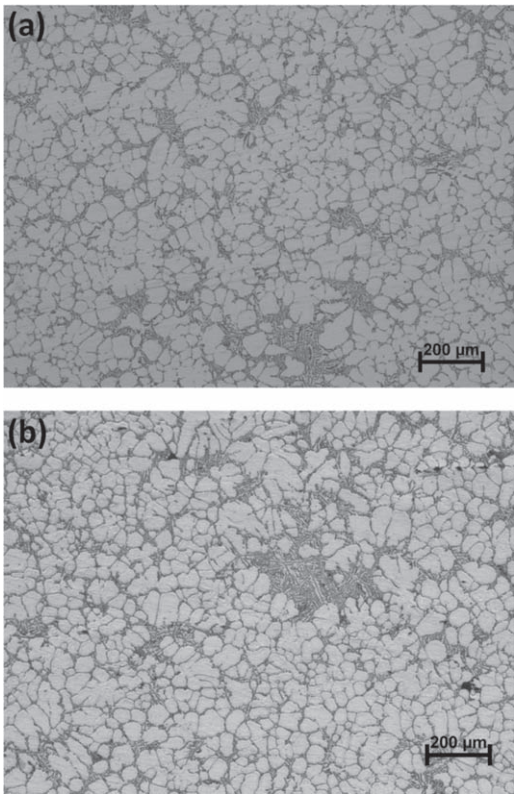


Figure 1. Microstructures of A356 as-cast ingots. (a) 30° and (b) 60° slope angles.

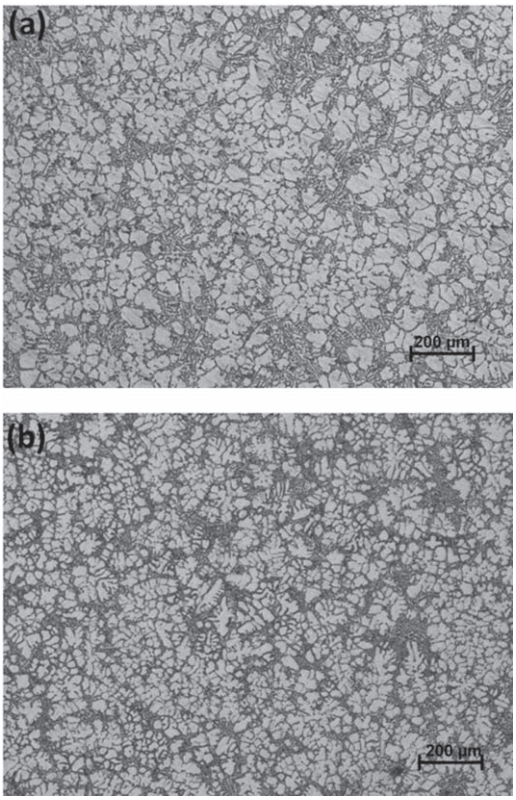
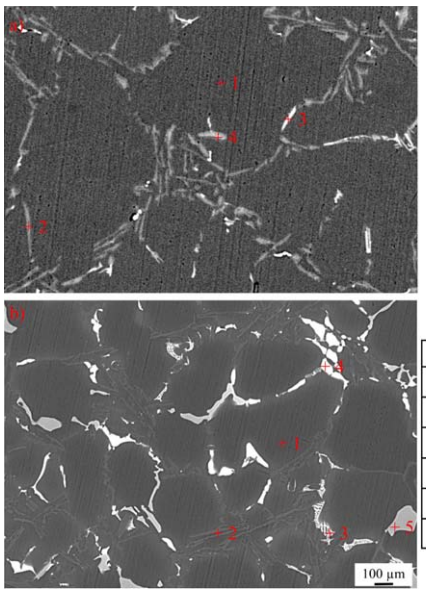


Figure 2. Microstructures of A380 as-cast ingots. (a) 30° and (b) 60° slope angles.

Table 2. Grain size, shape factor, and hardness of as-cast bars.

*	Grain Size (μm)	Shape Factor	Hardness (HB)
A356–30°	48.7	0.852	78.7
A356–60°	48.1	0.815	78.6
A380–30°	45.1	0.757	115.0
A380–60°	39.1	0.772	110.2



A356	Composition (wt%)			
Spot	Al	Si	Fe	Mg
1	100	-	-	-
2	56.38	43.62	-	-
3	73.05	14.86	3.29	8.80
4	72.42	18.50	9.08	-

A380	Composition (wt%)				
Spot	Al	Si	Fe	Cu	Mn
1	100	-	-	-	-
2	74.71	23.72	-	1.57	-
3	69.66	9.55	13.95	1.81	5.03
4	47.28	-	-	52.72	-
5	71.75	17.62	9.28	1.35	-

Figure 3. SEM images and EDS results of as-cast samples; (a) A356 and (b) A380.

The eutectic silicon in the casting microstructures occurred in the typical unmodified form. The cooling slope angle does not appear to have a significant effect on the eutectic structure in both alloys. The fact that the hardness of the alloys is at the same level depending on the slope angle also supports this situation. As can be seen from all these observations, the eutectic solidification starts in the steel mold, not on the cooling slope. Only the solidification of the α-Al phase starts on the surface of the cooling slope.

SEM images of the as-cast specimens are given in figure 3 with the related EDS results. Obtained results showed that colling slope as-cast specimens consist of common phases for both alloys. According to figure 3(a) as-cast A356 specimen consists of α-Al (spot 1), needle-like eutectic Si (spot 2), and two different intermetallics with Fe and Mg content (spots 3 and 4). On the other hand, according to figure 3(b) as-cast A380 specimen has the same α-Al and eutectic Si phases (spots 1 and 2) with more complex intermetallic constituents with Fe, Cu and Mn content (spot 3, 4 and 5).

XRD analysis was performed to determine these phases in the as-cast samples and the diffractograms are given in figure 4. The obtained XRD results indicate that α-Al, eutectic Si and β-Al_5FeSi phases coexist in both alloys. Owing to its higher Mg content, the $Al_8FeMg_3Si_6$ phase was found in A356 as-cast specimen and its morphology can be seen in figure 3(a) spot 3. On the other hand, $\alpha Al_{15}(Fe,Mn)_3Si_2$ and Al_2Cu were identified in the A380 as-cast sample as they were shown in figure 3(b) spot 3 and spot 4, respectively. In addition, the $AlMnCu_2$ phase was also identified through XRD analysis in A380 specimen however, it was not observed during SEM-EDS investigations.

The samples were cut from the casting bars were reheated in the semi-solid temperature zone for the same periods. Optic microscopy images of the microstructures of reheated samples produced with different tilt angles are given in figures 5 and 6, respectively.

In the scope of numerical analysis of microstructure images, grain size measurements and shape factor calculations were made and the obtained values are given in figures 7 and 8, respectively.

It is a physical fact that any heat treatment at high temperatures causes grain growth with the coalescence of similarly oriented grains and Ostwald ripening mechanism in further stages. During the reheating step, these two phenomena naturally take action in the growth of α-Al crystals. As can be seen in the results, grain growth commenced with the beginning of reheating, whereas sphericity increased especially over 20 min of reheating durations.

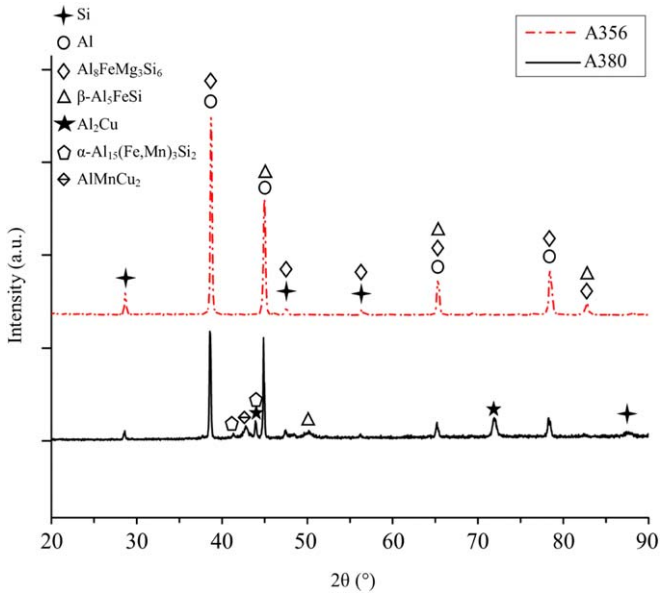


Figure 4. XRD patterns of as-cast samples.

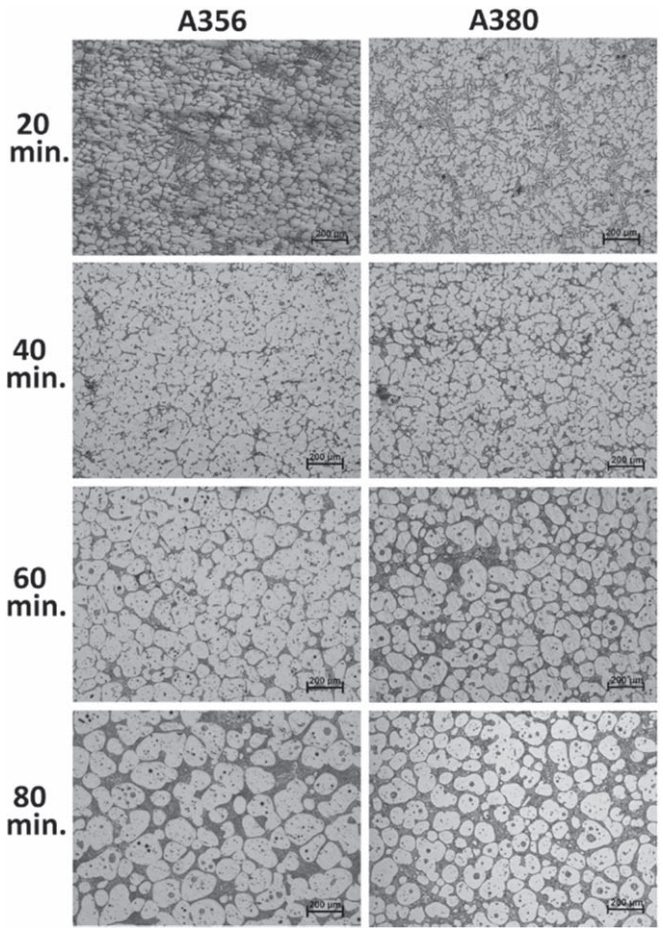


Figure 5. Microstructures of reheated samples cast with 30° of tilt angle.

In the case of reheating to the semi-solid zone, the liquid portion is formed by the melted eutectic. The α-Al grains grow spherically after surrounded by the liquid fraction. In this case, grains can grow easily in all directions. Therefore, it is not possible to discuss the formation of a significant liquid in the reheating for 20 min. The A356 alloy has a less complex microstructure than the A380 alloy, due to its simpler chemical composition.

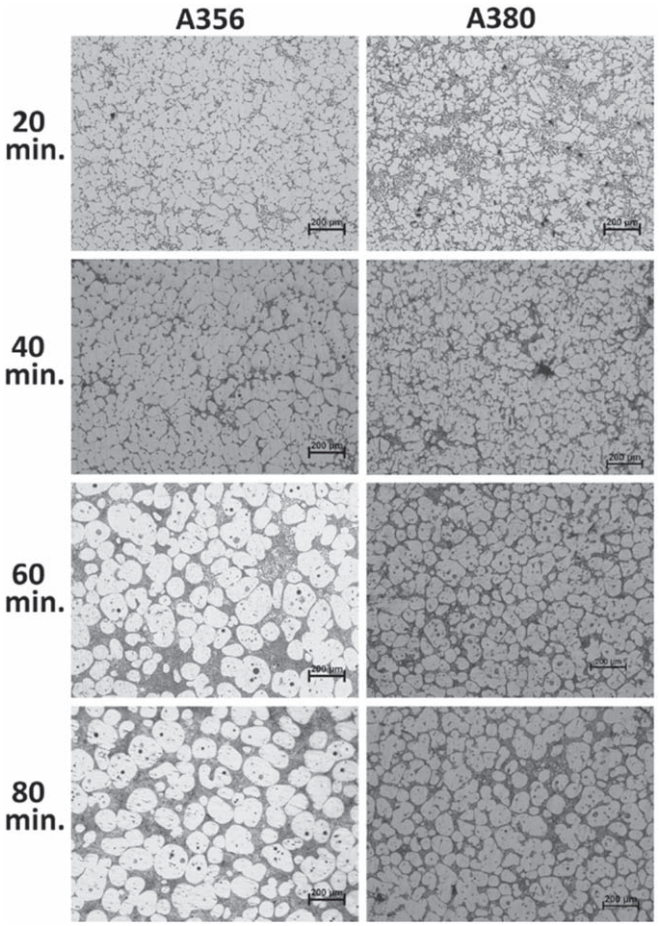


Figure 6. Microstructures of reheated samples cast with 60° of tilt angle.

The microstructural compounds of these two alloys were examined in detail in the former low superheat casting (LSC) and reheating studies [26].

While reheating causes the inevitable growth of α-Al grains, the amount of this situation was observed differently for two different alloys. Although A356 alloy had coarser microstructure in the as-cast state, the difference between the grain size of equally reheated specimens greatly expanded at the end of 80 min of reheating. The major difference between the grain growth behaviors of these two alloys is based on the differences in the thermal conductivity. At 25 °C, A356 alloy has a thermal conductivity of about 160 W/m.K, while this value is about 96 W/m.K for A380 alloy [27]. Due to its higher thermal conductivity, A356 alloy reacted faster to the heating process. This can be understood by the fact that the grain coarsening occurred more intensely alloy even during the reheating time of 20 min for A356 alloy.

Besides the growth and spheroidization of α-Al crystals, another major change was seen in the eutectic phase. Silicon needles in the unmodified eutectic structure of Al-Si alloys undergo gradual changes under the influence of heat. The first stage is disintegration, the second stage is the spheroidization, and the last stage is the growth in the matrix in polyhedral shape. In this study, since heating was done within the semi-solid range, a melting stage should be added to these. The disintegration of the eutectic silicon needles began at the reheating time of 20 min, and there is no sign of liquefaction in the microstructures within 20 min of heating. In the reheating time of 40 min, disintegration turned into the spheroidization and noticeable coarsening of grains started, also a small amount of liquid can be seen in the micrographs of 40 min reheated samples. The silicon growth in the reheating time of 60 min was observed in the polyhedral shape and a significant amount of melt eutectic was detected. Since the samples were quenched in water after the reheating process, the melted eutectic cooled very fast thus, solidified in a very fine morphology. Considering the ultra-fine eutectic regions appearing in the microstructures as a result of rapid solidification of liquefied eutectic, it gives information about the presence and amount of liquefaction in reheating. In figure 9, the polyhedral Si and fine eutectic structure are indicated on an enlarged image. Polyhedral silicon crystals in reheating time of 80 min continued to exist and the presence of polyhedral silicon crystals shows that the eutectic structure has not fully melted at the end of reheating.

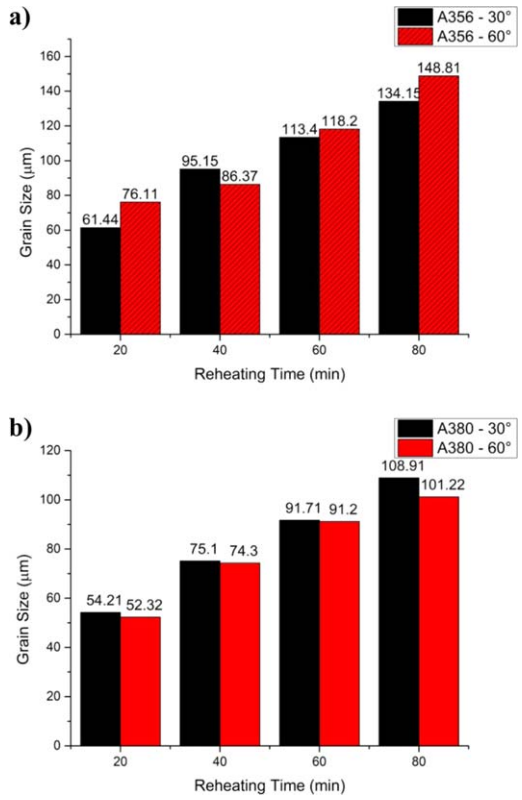


Figure 7. Grain size measurements for all reheated specimens; (a) A356 alloy, (b) A380 alloy.

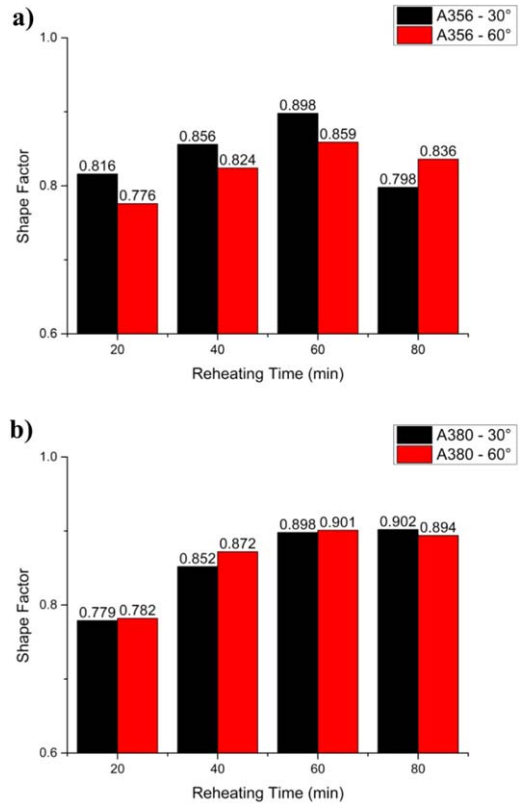


Figure 8. Shape factor calculations for all reheated specimen; (a) A356 alloy, (b) A380 alloy.

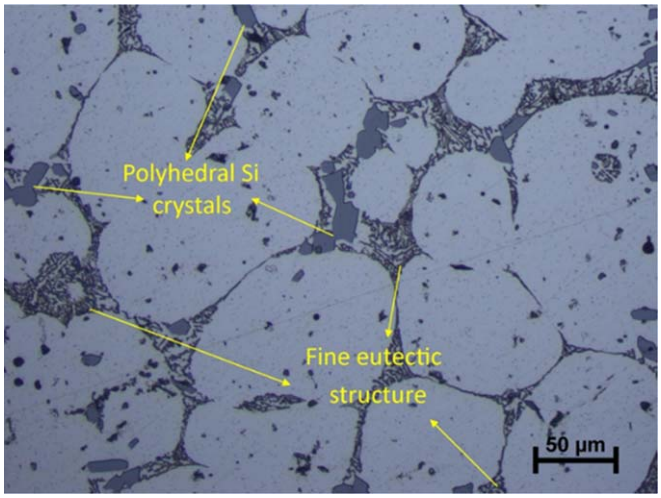


Figure 9. Coarse polyhedral Si crystals and fine eutectic structure solidified after quenching; micrograph belongs to 30° cast and 60 min reheated specimen of A356 alloy.

Table 3. Brinell hardness values of all reheated specimens (Unit of measurement is HB).

*	20 min	40 min	60 min	80 min
A356–30°	93.5	82.2	74.2	71.1
A356–60°	86.1	82.6	80.0	69.6
A380–30°	131.5	121.3	110.1	116.0
A380–60°	134.5	121.5	111.3	109.1

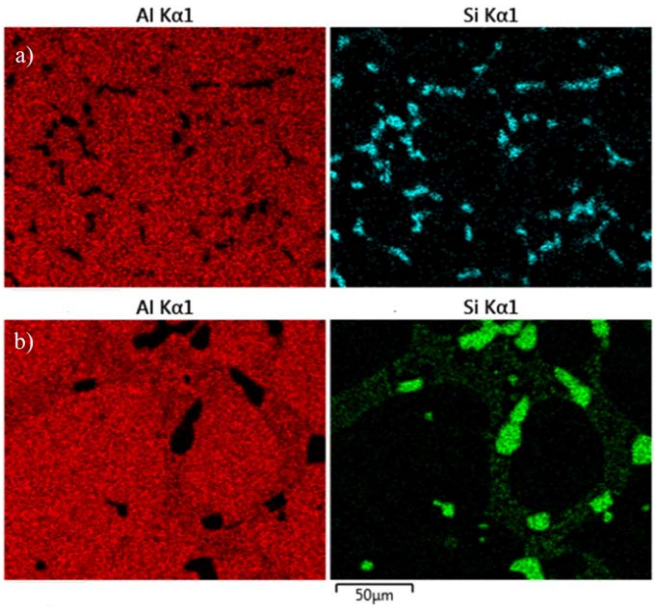


Figure 10. SEM-EDS elemental maps for Al and Si; (a) 40 min reheated A356 and (b) 80 min reheated A356 sample.

The hardness values of all reheated specimens are given in table 3. 20 min reheated samples displayed higher hardness values compared to the as-cast specimens despite the increased grain size due to the fact that eutectic Si morphology has crucial effects on mechanical properties for casting Al-Si alloys. The disintegration of the eutectic silicon resulted in an increase in hardness values until this point. However, a notable decrease followed with further reheating duration.

Continuation of the grain growth and coarsening of the silicon crystals started to reduce the hardness with 40 min of heating time. In the advancing process durations, the hardness continued to decrease due to the extensive grain growth and the merging of Si particles. However, the hardness values of A380 alloy seem to be equal to the hardness of the as-cast structure, on the other hand, the hardness values of A356 specimen with 80 min of reheating time were even below the hardness value of the as-cast specimen. SEM-EDS maps of the 40 and 80 min reheated A356 samples are given in figure 10 in order to better understanding the orientational and morphological changes on the eutectic Si. In the 40 min reheated samples it was observed that Si particles created a network through the grain boundaries and the coarsening was limited. The Si network was also observed in the 80 min reheated sample but the elemental content mostly shifted into the coarse polyhedral Si particles. Therefore, a significant decrease in hardness has become inevitable with grain growth and this formation.

4. Conclusion

In this study, specimens of two different Al-Si casting alloy were produced with CS casting with different tilt angles and reheated at different times. Microstructural and hardness properties of the as-cast and reheated specimens were investigated and the main conclusions can be listed as follows:

(1) The CS casting method was observed as an efficient method for producing suitable non-dendritic feedstocks for the semi-solid forming of Al-Si casting alloys.

(2) Chemical compositions of the alloys were found effective in the grain sizes and the tilt angle did not show any crucial effect on the microstructures. As it provided a slightly finer casting structure for A380 alloy, the slope angle of 60° can be preferred over 30°. On the other hand, A356 alloy did not display any characteristic behavior depending on the casting angle, but it is preferable to choose a casting angle of 60° for the possibility of less residual shell formation on the slope surface. Thus, casting efficiency can be maximized.

(3) In addition to the growth and spheroidization of the α-Al phase during the reheating process, the changes in the eutectic phase were found noteworthy too. Considering the effects of these changes on the hardness properties, naturally, other mechanical properties will also be affected.

(4) The thermal properties of the alloys were seemed to be effective in the course of development of microstructural compounds.

(5) Reheating is certainly the most important step in the thixoforming processes. There are many factors to be considered when determining the reheating time and temperature. Slug dimensions, heating technique, desired liquid content, degree of forming and the desired final properties are the major ones. With the selected reheating temperatures and durations, the developments in A356 and A380 alloys are generally explained in this study. However, it should be noted that each process will have its own specific conditions.

ORCID iDs

Serhat Acar https://orcid.org/0000-0003-1732-4995

References

[1] Atkinson H V 2010 Semisolid processing of metallic materials *Mater. Sci. Technol.* **26** 1401–13
[2] Salleh M S, Omar M Z, Syarif J and Mohammed M N 2013 An overview of semisolid processing of aluminium alloys *ISRN Mater. Sci.* **2013** 1–9
[3] Kumar S D, Mandal A and Chakraborty M 2014 Cooling slope casting process of semi-solid aluminum alloys: a review *Int. J. Eng. Res. Technol.* **3** 269–83 https://www.ijert.org/research/cooling-slope-casting-process-of-semi-solid-aluminum-alloys-a-review-IJERTV3IS070312.pdf
[4] Atkinson H V and Liu D 2008 Microstructural coarsening of semi-solid aluminium alloys *Mater. Sci. Eng.* A **496** 439–46
[5] Alhawari K S, Omar M Z, Ghazali M J, Salleh M S and Mohammed M N 2015 Evaluation of the microstructure and dry sliding wear behaviour of thixoformed A319 aluminium alloy *Mater. Des.* **76** 169–80
[6] Hassas-Irani S B, Zarei-Hanzakz A, Bazaz B and Roostaei A A 2013 Microstructure evolution and semi-solid deformation behavior of an A356 aluminum alloy processed by strain induced melt activated method *Mater. Des.* **46** 579–87
[7] Robert M H, Zoqui E J, Tanabe F and Motegi T 2007 Producing thixotropic semi-solid A356 alloy: microstructure formation x forming behaviour *J. Achiev. Mater. Manuf. Eng.* **20** 19–26 https://www.infona.pl/resource/bwmeta1.element.baztech-article-BOS5-0018-0001
[8] Jiang J, Wang Y and Atkinson H V 2014 Microstructural coarsening of 7005 aluminum alloy semisolid billets with high solid fraction *Mater. Charact.* **90** 52–61
[9] Atkinson H V 2005 Modelling the semisolid processing of metallic alloys *Prog. Mater Sci.* **50** 341–412

[10] Bolouri A, Shahmiri M and Cheshmeh E N H 2010 Microstructural evolution during semisolid state strain induced melt activation process of aluminum 7075 alloy *Trans. Nonferrous Met. Soc. China* **20** 1663–71
[11] Jiang J, Wang Y, Xiao G and Nie X 2016 Comparison of microstructural evolution of 7075 aluminum alloy fabricated by SIMA and RAP *J. Mater. Process. Tech.* **238** 361–72
[12] Haga T and Kapranos P 2002 Billetless simple thixoforming process *J. Mater. Process. Tech.* **130–131** 581–6
[13] Das P, Samanta S K, Venkatpathi B R K, Chattopadhyay H and Dutta P 2012 Microstructural evolution of A356 Al alloy during flow along a cooling slope *Trans. Indian Inst. Met.* **65** 669–72
[14] Thuong N, Zuhailawati H, Seman A A, Huy T D and Dhindaw B K 2015 Microstructural evolution and wear characteristics of equal channel angular pressing processed semi-solid-cast hypoeutectic aluminum alloys *Mater. Des.* **67** 448–56
[15] Qin Q D, Zhao Y G, Cong P J, Zhou W and Xu B 2007 Semisolid microstructure of Mg2Si/Al composite by cooling slope cast and its evolution during partial remelting process *Mater. Sci. Eng.* A **444** 99–103
[16] Taghavi F and Ghassemi A 2009 Study on the effects of the length and angle of inclined plate on the thixotropic microstructure of A356 aluminum alloy *Mater. Des.* **30** 1762–7
[17] Mahmoud T S, El-Kady E Y, Zakaria H M, El-Awady A and El-Sherbiny M F 2016 Optimization of the low superheat casting process parameters for producing of thixotropic A356 alloy feedstock *Mater. Sci. An Indian J.* **14** 246–54 https://www.tsijournals.com/articles/optimization-of-the-low-superheat-casting-process-parameters-for-producing-of-thixotropic-a356-alloy-feedstock.pdf
[18] Khosravi H, Eslami-Farsani R and Askari-Paykani M 2014 Modeling and optimization of cooling slope process parameters for semi-solid casting of A356 Al alloy *Trans. Nonferrous Met. Soc. China* **24** 961–8
[19] Haga T and Suzuki S 2001 Casting of aluminum alloy ingots for thixoforming using a cooling slope *J. Mater. Process. Technol.* **118** 169–72
[20] Legoretta E C, Atkinson H V and Jones H 2008 Cooling slope casting to obtain thixotropic feedstock II: observations with A356 alloy *J. Mater. Sci.* **43** 5456–69
[21] Birol Y 2007 A357 thixoforming feedstock produced by cooling slope casting *J. Mater. Process. Technol.* **186** 94–101
[22] Das P, Samanta S K, Das R and Dutta P 2014 Optimization of degree of sphericity of primary phase during cooling slope casting of A356 Al alloy: Taguchi method and regression analysis *Measurement* **55** 605–15
[23] Samat S, Omar M Z, Mohamed I F, Sajuri Z, Aziz A M and Arif M A M 2019 Thixoformability and microstructural evolution of Al-Si-Cu alloys *Mater. Today Proc.* **17** 1161–8
[24] Kolahdooz A and Dehkordi S A 2019 Effects of important parameters in the production of Al-A356 alloy by semi-solid forming process *J. Mater. Res. Technol.* **8** 189–98
[25] Tenekedjiev N, Mulazimoglu H, Closset B and Gruzleski J 1995 *Microstructures and Thermal Analysis of Strontium-Treated Aluminum-Silicon Alloys* 1st edn (Illinois: American Foundrymen's Society)
[26] Gecu R, Acar S, Kisasoz A, Guler K A and Karaaslan A 2018 Influence of T6 heat treatment on A356 and A380 aluminium alloys manufactured by thixoforging combined with low superheat casting *Trans. Nonferrous Met. Soc. China* **28** 385–92
[27] ASM handbook volume 2 1990 *Properties and Selection: Nonferrous Alloys and Special-Purpose Materials* 10th edn (Ohio: ASM International)